

Surface-Plasmon-Mediated Hydrogenation of Carbonyls Catalyzed by Silver Nanocubes under Visible Light

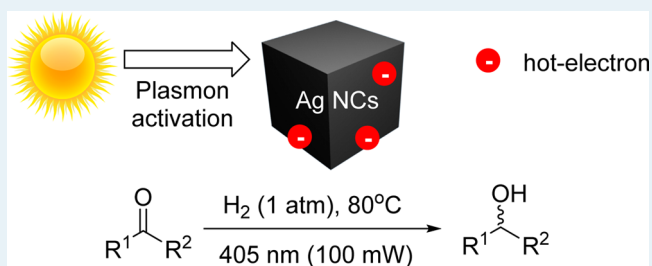
Michael J. Landry, Alexandra Gellé, Beryl Y. Meng, Christopher J. Barrett, and Audrey Moores*[✉]

Department of Chemistry, McGill University, 801 Sherbrooke Street West, Montréal, QC H3A 0B8, Canada

S Supporting Information

ABSTRACT: Plasmonic nanoparticles are exciting and promising candidates for light-activated catalysis. We report herein the use of plasmonic nanocubes for the activation of molecular hydrogen and the hydrogenation of ketones and aldehydes via visible light irradiation at 405 nm, corresponding to the position of the plasmon band of the nanocubes, at 80 °C. Only 1 atm of molecular hydrogen is required to access, using catalytic amounts of silver, primary, and secondary alcohols, with complete chemoselectivity for C=O over C=C reduction. The resulting catalytic system was studied over a scope of 12 compounds. Exposure to other wavelengths, or absence of light failed to provide activity, thus proving a direct positive impact of the plasmonic excitation to the catalytic activity. By varying the irradiation intensity, we studied the relationship between plasmon band excitation and catalytic activity and propose a potential reaction mechanism involving plasmon-activated hot electrons. This study expands the scope of reactions catalyzed by free-standing plasmonic particles and sheds light on H₂ activation by silver surfaces.

KEYWORDS: photocatalysis, silver nanoparticles, hydrogenation, plasmonic catalysis, surface plasmon resonance



Energy consumption by the chemical industry is a significant source of pollution via generation of greenhouse gases.^{1–3} Photochemical reactions have been investigated for over a century, with the end-goal of harvesting light as a renewable energy source and converting it directly into chemical energy.⁴ Photochemistry can also open routes to products which are not accessible via thermal routes.⁵ Energy transfer is a key step in being able to use light to do meaningful chemical work, and to this end, several light-harvesting systems have been developed, including solar cell materials,⁶ photocatalysts,^{7–9} and photoactivated materials,¹⁰ relying on materials such as TiO₂,^{11,12} porphyrin dyes,^{13,14} ruthenium polypyridine complexes,^{15–17} or organic dyes.^{18,19} Light-activated catalytic reactions have seen wide use in organic chemistry⁸ and also in remediation and depollution of organic dyes and conjugated organic systems.²⁰ Recent efforts have allowed the development of such photocatalysts with a focus on activation with visible light.²¹

Nanomaterials of Cu, Ag, and Au possess an optical and electronic property called surface plasmon resonance (SPR), which confers to them powerful absorptive properties in the visible region. Conducting electrons in these materials oscillate in resonance with the incoming light field,^{22–24} causing three effects. (1) SPR causes strong light absorption and scattering translating into exciting optical properties.^{25,26} (2) Strong field enhancement at the surface vicinity of these materials allows them to enhance signals, and was exploited to develop surface enhanced Raman spectroscopy (SERS) used for detection with molecular sensitivity.^{27–32} (3) Field enhancement also causes

local heat generation and this has been used in the development of nanomedicines.^{27,33,34} In the last 10 years, researchers have studied light-mediated catalysis using SPR-active nanoparticles (SPRANP), including for water splitting, CO₂ reduction, and organic pollutant degradation.^{21,23,35–39} SPRANP operate according to three major schemes: their plasmon is enabled by visible light and they either activate a metal oxide support, another metal, or act as a catalyst on their own (Scheme 1). For instance, Au nanoparticles (NPs) supported on oxides have been shown to catalyze the oxidation of formaldehyde,³⁸ alcohols,^{40–43} and amines to imines,^{44–46} C–C and amine–alkyne–aldehyde couplings,^{46,47} hydroamination of alkynes,⁴⁶ oxidative degradation of phenol,⁴⁸ oxidative aldehyde–amine condensation to amide,⁴⁹ and hydroxylation of benzene.^{50–52} In supported SPRANP, oxidative reactions are mediated by excited hot electrons from SPRANP which are transferred to the support where catalysis takes place (Scheme 1).^{21,38}

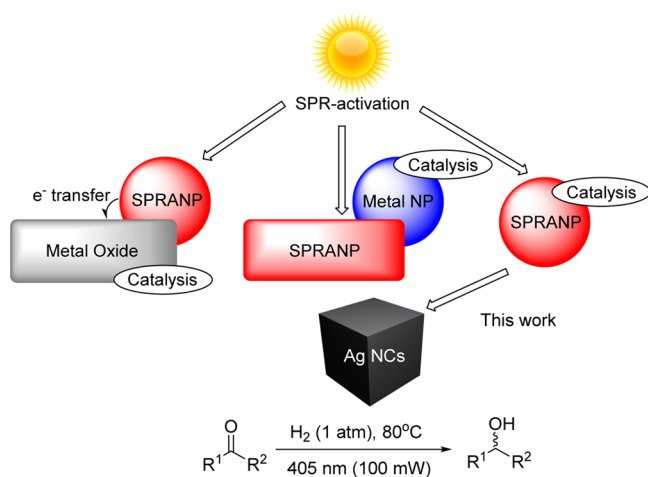
Researchers have looked into combining the catalytic activity of nonplasmon active transition metals, such as Pt or Pd with optical properties of SPRANP. For instance, alloys of plasmon and nonplasmon metals were investigated.^{46,53,54} Besides this, Halas and co-workers unraveled the potential of a less-explored plasmonic metal: aluminum.^{55,56} Core–shell Al/Al₂O₃ nanocrystals were used as supports for Pd NPs, for the selective

Received: June 28, 2017

Revised: August 7, 2017

Published: August 9, 2017

Scheme 1. General Categories of Plasmonic Photocatalysts Relying on SPRANP



hydrogenation of acetylene to ethylene under white-light illumination.⁵⁶ Typical reactions such as ethanol dehydrogenation can be enhanced with such core–shell particles.⁵⁷ On the other end, free-standing, pure SPRANP can also perform plasmonic photocatalysis, for instance in oxidative couplings,^{58,59} activations of reagent gases,⁶⁰ and reductive couplings.⁶¹ The Scaiano group showed the reduction of alcohol with hydrogen peroxide with unsupported Au NPs.⁶² The group of Lincic looked at Cu NPs as SPR-activated propylene oxidation catalysts.⁶³ The same group explored silver nanocubes (Ag NCs) harvesting light via SPR to directly afford hot electrons and catalyze the epoxidation of ethylene.⁵³ In an effort to explore more the scope of catalytic processes available from pure silver as a plasmonic metal, we wanted to look at their reductive chemistry in organic solvents. Hydrogenation is a reaction of high industrial relevance,⁶⁴ for which silver is typically a less active metal requiring high hydrogen pressure; its limited ability to activate H₂ compared to other metals is well-documented.⁶⁵ Still it affords heterogeneous catalysts with excellent chemoselectivity for the reduction of C=O over C=C bonds.^{65–69} Au NPs, both in the free and supported versions, are known to enable the activation of molecular hydrogen via SPR,^{70,71} but a similar effect had not been shown yet for silver. Activating silver toward H₂ splitting can help reduce the high temperature and pressure requirements for this reaction.

Herein, we report that plasmonic Ag NCs are able to drive catalytic reduction reactions and direct activation of H₂ through the absorption of visible light, at ambient pressure. This expands the use of catalytic plasmonic nanoparticles to reductive organic chemical transformations, where it has been less explored.

For this work, Ag NCs were selected for their enhanced SPR properties arising from their sharp vertices.^{72,73} These sharp vertices are well-known to create “hot spots” where SPR is greatly enhanced.^{23,35} We synthesized Ag NCs following the procedure already reported, using AgNO₃ as a precursor, polyvinylpyrrolidone (PVP) as a stabilizer, and HCl as an etchant.⁵⁵ Transmission electron microscopy (TEM) and scanning electron microscopy (SEM) (Figures 1, S2–S4) revealed that most of the synthesized nanoparticles featured a cubic morphology, with occasionally a few rod- or prism-shaped particles observed. These cubes are monodisperse with an average edge length of 126 ± 12 nm (counted over 120 cubes

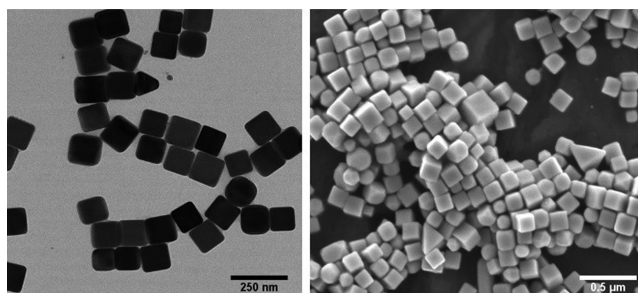


Figure 1. TEM (left) and SEM (right) images of Ag NCs.

in TEM images). In STEM, the shell of protective PVP polymer was clearly visible (Figure S4). Dynamic light scattering (DLS) experiments were also performed and results are consistent with SEM and TEM data (See Supporting Information). Energy-dispersive X-ray spectroscopy (EDS) measurements were obtained on Ag NCs imaged by STEM to probe their purity (Figure S5). Ag NCs were found to contain only Ag, Cl, C, and O. Importantly no other noble metals (Pt, Pd, or Ru), which could also lead to the expected reduction chemistry, was detected. An EDS linescan was also performed across a couple of AgNCs observed by high resolution STEM (Figure S6). Carbon and oxygen were preeminent along the edges of the cubes, revealing the surface coverage of the PVP polymer. The presence of chlorine revealed by EDS was consistent with the Ag NC synthesis, which relies on chloride anions in order to direct the selective facet growth of the cubes. X-ray photoelectron spectroscopy (XPS) confirmed the presence of Ag, Cl, C, O, and N in the sample. Cl content could be quantified against Ag and Cl and accounts for 8% of the inorganic material (Figure S7). The 3d_{5/2} band of silver, centered at 368.3 eV is consistent with Ag(0). X-ray diffraction (XRD) featured (111) and (200) peaks distinctive of a pure Ag(0) phase (Figure S9).⁷⁴ The surface plasmon band (SPB) was measured using UV–vis spectroscopy and was determined to lie centered at 410 nm (Figure 2).

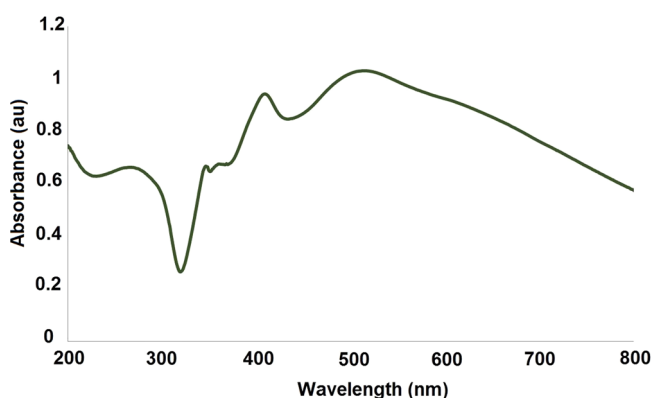


Figure 2. UV–vis spectrum of Ag NCs that demonstrates the surface plasmon band ranging from 400–420 nm.

To establish catalytic activity, the Ag NCs were first tested for the hydrogenation of camphor to the diastereotopic mixture of borneol and isoborneol, using a hydrogen pressure of 1 atm for 24 h (Figure 3). Camphor was selected as model substrate for this reaction because, in the presence of light, it does not form photoradicals as other arylketones are known to do. When this reaction was performed under 1 atm of H₂ in the dark, at

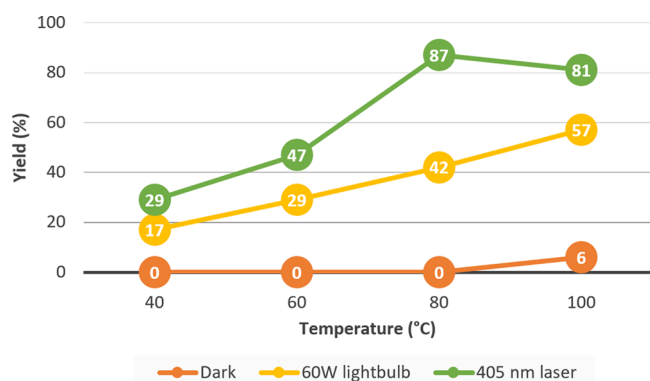


Figure 3. Yields observed for the hydrogenation of camphor with Ag NCs as catalyst. Reaction conditions: 1 mg of Ag NCs, 1 mmol of camphor and 5 mL of dioxane, H₂ pressure of 1 atm, 24 h.

40 or 60 °C, no conversion was measured after 24 h. Further heating at 80 or 100 °C afforded only trace or 6% conversions respectively under the same conditions (Figure 3). This is consistent with past accounts, as typically much higher pressures of molecular hydrogen (i.e., 40 bar) are required to trigger hydrogenation with silver nanoparticles.^{66,75} However, when light from a 60 W lightbulb was introduced during the reaction, a promising increase in yield of 17% was measured at 40 °C. Upon raising the temperature, the yields improved further and reached 57% at 100 °C. In order to further ascribe this activity enhancement to the Ag NCs SPR properties, we employed a laser diode emitting light precisely at 405 nm, a wavelength within their plasmon band. The typical experimental setup for this reaction is illustrated in Figure S1. A dramatic improvement of yield was observed using the 405 nm laser, enhancing the yield to 87%, an increase of 45 points compared to the wide-spectrum light bulb of similar intensity (Figure 3). A series of control tests established that absence of H₂, absence of particles or exposure to 532 or 633 nm laser light failed to afford meaningful conversions, under the temperature spectrum explored herein (Table S2).

Now that a link between light and catalytic activity was established, a solvent screening was performed to understand the impact of the polarity on the reaction. Dioxane, water, ethanol, hexane, ethyl acetate, and dichloromethane were assessed under the newly optimized conditions (H₂ pressure of 1 atm, 24 h) at their boiling point, or at 40 °C. We correlated the resulting yields (Table S3) with the solvent dielectric constant, ϵ , a classic parameter used to measure polarity and boiling temperature. Interestingly, a clear trend was observed, where the more polar the solvent, the better the activity (Figure S10 and S11). Dioxane and water performed the best, achieving similar yields of near 80% at 100 °C. The case of dioxane is interesting: while this molecule has a dielectric constant of zero because of its high symmetry, it possesses polar bonds, which have a local polarizing effect on the medium. Similar results have been reported by others, where dioxane performed very well and similarly to polar solvents for C=O hydrogenation.⁷⁶ Ethanol only provided 30% conversion at 78 °C, a temperature at which dioxane afforded the excellent yield of 87%. All other solvents, all apolar, gave poor yields.

To probe further into the photocatalytic nature of this reaction, a light intensity versus yield experiment was conducted. Under optimized reaction conditions (H₂ pressure of 1 atm, 24 h, 80 °C), the 405 nm laser was expanded to the

size of the reaction vessel, and used at its full intensity of 204 mW/cm², then also under reduced intensities stepwise by employing various increasing optical density (OD) neutral density filters. As shown in Figure 4, below 60 mW/cm² the

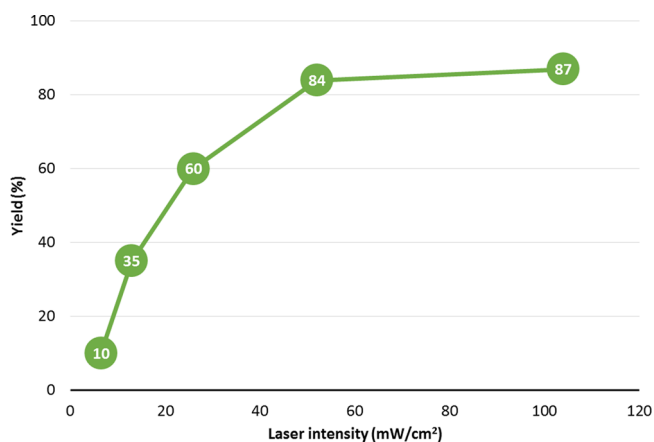
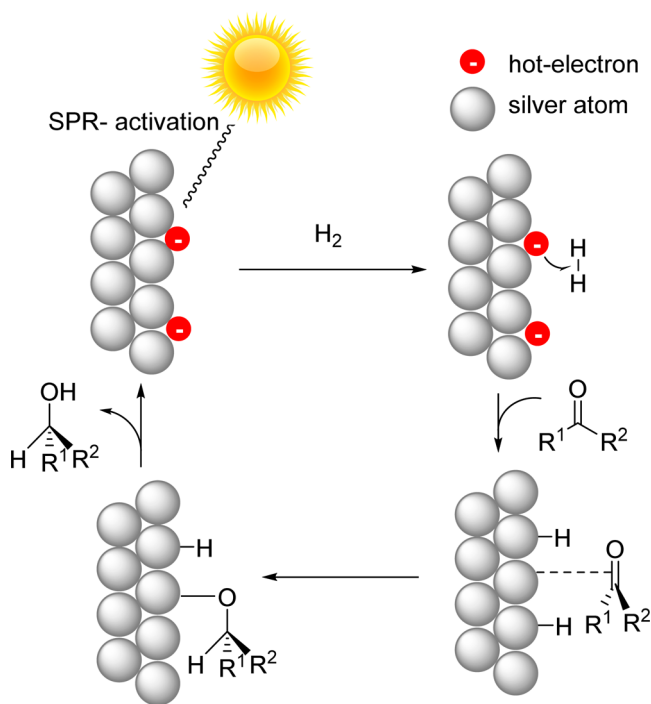


Figure 4. Yield (%) vs laser intensity (mW/cm²) for the hydrogenation of camphor with Ag NCs as catalyst in dioxane, with H₂ pressure of 1 atm, 80 °C and for 24 h.

yield increased almost linearly as a function of light intensity, while after this value, a saturation was rapidly established. This saturation can be explained potentially by diffusion limitations in a solution-based catalytic process, when yields exceed 50%. A kinetic study was also carried out using camphor as the model reaction under hydrogen conditions. A mostly linear loss of camphor was observed, without induction period (Figure S12).

Unsupported SPRANP have been described to enable plasmonically enhanced catalysis via three main mechanisms:^{23,24} (i) the formation of hot electron–hole pairs at the surface of the nanoparticle, followed by transfer of charge carriers to an adsorbed substrate, (ii) the photoinduced increase of the nanoparticle temperature and its thermal effects on the reaction rate, (iii) the photoinduced local field enhancement and its effect on other photoactivated processes. The reaction of hydrogenation with silver does not proceed via photo excitation of an organic molecule involved, so a field enhancement effect (iii) is unlikely. Also, since reaction with Ag NCs in the dark was negligible across the range of temperatures accessible in the liquid phase of dioxane, a potential thermal effect of the SPR (ii) should not lead to activity enhancement. Thermal effects are also typically encountered with nanoparticles much smaller than the ones we used.³⁵ The dependence of the yield on the light intensity before saturation is also in agreement with a linear relationship, consistent with a “hot-electron” process for low intensity photoactivation.⁷⁷ Recently, the group of Halas demonstrated the activation of H₂ by gold nanoparticles under plasmonic activation, and they proposed that hot electrons are directly responsible for the splitting of the H₂ molecule.⁷¹ Thus, we propose a similar mechanism in Scheme 2. When light is absorbed by the Ag NCs, a transient electron/hole pair is formed at its surface and the resulting hot electron is transferred to an adsorbed H₂ molecule. The rest of the proposed mechanism follows a Polanyi-Horvut scheme.⁷⁸ Interestingly, it has been suggested by theoretical investigations that hydrides on silver surfaces may be directly photoactivated by SPR, which could participate as well in the process.⁷⁹

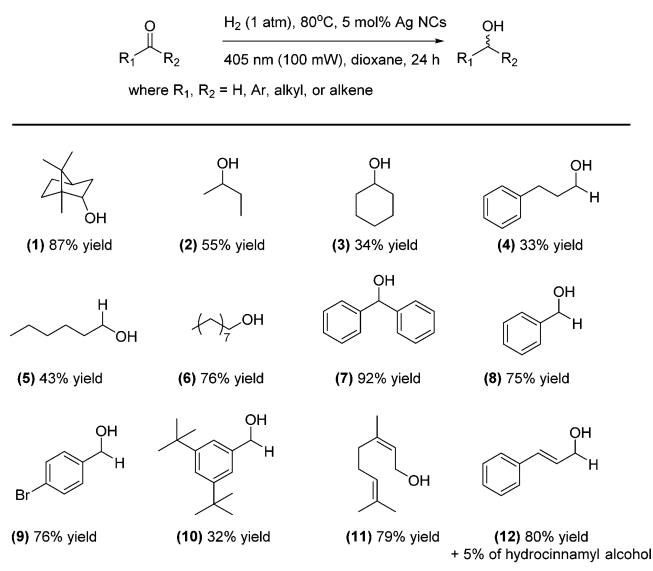
Scheme 2. Proposed Mechanism for the Hydrogenation of Carbonyl Compounds with H₂ Catalyzed by Ag NCs



Moreover, AgCl and Ag@AgCl NCs have been reported by others to be active photocatalysts in polymerization and oxidation reactions and it was important to rule out the presence of any AgCl phase in as-synthesized nanocatalysts.^{80–82} XRD did not show any sign of crystalline AgCl phase, and no typical AgCl UV signature was seen between 200 and 300 nm (Figure 2).

With these results in hand, the scope of this reaction was explored with other ketones and aldehydes (Scheme 3), setting the temperature to 80 °C and using the 405 nm laser as the irradiation source. Camphor (**1**), for which we optimized the reaction gives a yield of 87%. Other aliphatic ketones gave the

Scheme 3. Scope of Products Obtained from SPR-Enhanced Hydrogenation of Ketones with Ag NCs



corresponding alcohol (**2–3**) in moderate yields, with percentages in the 30s and 50s of %. Aliphatic aldehydes afforded contrasted results with yields between 33% and 76% for (**4**) to (**6**). Moving to conjugated carbonyl molecules, we observed better yields, consistent with their known enhanced reactivity toward hydrogenation. Benzophenone gives (**7**) with the best yields of the series (92%) and good yields around 75% are seen for benzyl-alcohol (**8**) and its *p*-chloro counterpart (**9**). Perfect selectivity for (**9**) shows the tolerance of the procedure for chloroarene functionality. The di-*m-t*-butyl benzyl-alcohol (**10**) affords a low yield of 32% likely because of steric bulk which can hinder access to the metal nanoparticle surface. In the example of α,β -unsaturated aldehydes, we observe an interesting selectivity for the C=O bond reduction over the C=C bond, consistent with past accounts using Ag NPs for hydrogenation.⁷⁵ Citral is thus cleanly converted to geraniol (**11**) at 79% yield. With cinnamaldehyde, 80% yield of cinnamyl alcohol (**12**) was produced, along with 5% of hydrocinnamyl alcohol.

To elucidate the potential leaching of soluble Ag species during the reaction, ICP-MS measurements were performed on the filtrate of the optimized hydrogenation reactions of camphor, after Ag NC removal. 0.57 ppm of Ag was measured in the product, which constitutes a negligible contamination (see Supporting Information). In an effort to determine if such leached soluble Ag species were responsible for catalytic reactivity, we performed two distinct experiments: a hot filtration and a blank test using AgNO₃ as catalyst. For the hot filtration, an optimized catalytic run was performed at 80 °C, with laser excitation. After 2 h, the Ag NCs were filtered off the reaction medium, and the run was further monitored for activity, under the same conditions for 6 additional hours. Before the separation, a yield of 21% conversion to borneol was measured. At the end of the run, a similar yield of 23% was obtained. We also performed a reaction using AgNO₃ as catalyst, added to the reaction at a concentration of 0.57 ppm. This blank test afforded only trace conversion over the 24 h along with the appearance of a silver mirror on the side of the flask, characteristic of Ag(0). Homogenous Ag species have been reported recently to be active for hydrogenation, but require much higher loadings, H₂ pressures, and electron-accepting ligands.⁶⁹ These tests established that soluble species can not account for the reactivity described in this study.

In an effort to explore organic reactions catalyzed by SPR-activated Ag NCs, we also investigated the oxidation of aldehydes and alcohols to carboxylic acids. Ag NCs are known to activate O₂ with SPR and enable gas-phase epoxidation of alkenes.⁵³ For this study, we explored the oxidation of *p*-hydroxybenzaldehyde under air at atmospheric pressure for 18 h at 60 °C. Under these conditions, the corresponding carboxylic acid is produced at 95% under 405 nm laser irradiation, or using a light bulb, while in the dark this value falls to 34%. A scope of six molecules was explored and found yield values between 65% and 97% (Figure S13). Similar conditions were also tested for the direct oxidation of alcohols to carboxylic acids. Under the conditions we tested, we did observe a small activity, but we could not secure yields beyond 11% (Figure S14).

These results demonstrate that SPR can be harnessed to activate silver toward hydrogenation of carbonyl compounds. SPR-activated silver-catalyzed hydrogenation proceeded smoothly at 1 atm of H₂ and 80 °C, conditions much milder than what is known for purely thermal silver-catalyzed

processes. This reaction is the first example of SPR-activated reductive catalysis performed using pure, unmodified plasmonic nanoparticles. This catalyst has been shown to tolerate a wide variety of substrate scopes with moderate to high yields, with complete selectivity for C=O vs C=C double bond reduction. Kinetic studies, dose/response curves, solvent dependence, and complete Ag NCs characterization were combined to propose a mechanism via light-induced hot electron formation. This work is a proof-of-concept of the use of plasmon-active nanocatalysts for important organic transformations.

■ ASSOCIATED CONTENT

● Supporting Information

The Supporting Information is available free of charge on the ACS Publications website at DOI: [10.1021/acscatal.7b02128](https://doi.org/10.1021/acscatal.7b02128).

Detailed experimental section and complete characterization data of SEM, TEM, bright field scanning transmission microscopy (BFSTEM), EDS, XRD, XPS, DLS, UV-vis (PDF)

■ AUTHOR INFORMATION

Corresponding Author

*Tel: +1 (514) 398-4654, Fax: +1 (514) 398-3797, E-mail: audrey.moore@mcgill.ca.

ORCID

Audrey Moores: [0000-0003-1259-913X](https://orcid.org/0000-0003-1259-913X)

Notes

The authors declare no competing financial interest.

■ ACKNOWLEDGMENTS

We are grateful to Dr. David Liu for the help with TEM and SEM images, to Ms. Mary Bateman for the help with ICP, to Mr. Nicolas Brodusch for BFSTEM imaging and EDS analysis, to Mr. Louis Do for his help with the XRD measurements and to Dr. Madhu Kaushik for the help with GCMS. We thank the Natural Science and Engineering Research Council of Canada (NSERC) Discovery Grant program, the Canada Foundation for Innovation (CFI), the Canada Research Chairs (CRC), the Centre for Green Chemistry and Catalysis (CGCC), NSERC-Collaborative Research and Training Experience (CREATE) in Green Chemistry, and McGill University for their financial support.

■ REFERENCES

- (1) Burnham, A.; Han, J.; Clark, C. E.; Wang, M.; Dunn, J. B.; Palou-Rivera, I. *Environ. Sci. Technol.* **2012**, *46*, 619–627.
- (2) Searchinger, T.; Heimlich, R.; Houghton, R. A.; Dong, F.; Elobeid, A.; Fabiosa, J.; Tokgoz, S.; Hayes, D.; Yu, T.-H. *Science* **2008**, *319*, 1238–1240.
- (3) Franzén, R.; Xu, Y. *Can. J. Chem.* **2005**, *83*, 266–272.
- (4) Ciamician, G. *Science* **1912**, *36*, 385–394.
- (5) Svoboda, J.; König, B. *Chem. Rev.* **2006**, *106*, 5413–5430.
- (6) Ding, G.; Jin, Q.; Chen, Q.; Hu, Z.; Liu, J. *Nanoscale Res. Lett.* **2015**, *10*, 491.
- (7) Yoon, T. P.; Ischay, M. A.; Du, J. *Nat. Chem.* **2010**, *2*, 527–532.
- (8) Lin, S.; Ischay, M. A.; Fry, C. G.; Yoon, T. P. *J. Am. Chem. Soc.* **2011**, *133*, 19350–19353.
- (9) Luo, J.; Zhang, J. *ACS Catal.* **2016**, *6*, 873–877.
- (10) Ye, X.; Kuzyk, M. G. *Opt. Commun.* **2014**, *312*, 210–215.
- (11) Fujishima, A.; Rao, T. N.; Tryk, D. A. *J. Photochem. Photobiol., C* **2000**, *1*, 1–21.
- (12) Sakthivel, S.; Kisch, H. *Angew. Chem., Int. Ed.* **2003**, *42*, 4908–4911.
- (13) Wang, Z.; Medforth, C. J.; Shelnutz, J. A. *J. Am. Chem. Soc.* **2004**, *126*, 16720–16721.
- (14) Minoura, N.; Tsukada, M.; Nagura, M. *Biomaterials* **1990**, *11*, 430–434.
- (15) Wang, P.; Zakeeruddin, S. M.; Moser, J. E.; Nazeeruddin, M. K.; Sekiguchi, T.; Grätzel, M. *Nat. Mater.* **2003**, *2*, 402–407.
- (16) Windle, C. D.; Perutz, R. N. *Coord. Chem. Rev.* **2012**, *256*, 2562–2570.
- (17) Narayanam, J. M. R.; Stephenson, C. R. J. *Chem. Soc. Rev.* **2011**, *40*, 102–113.
- (18) Neumann, M.; Fuldner, S.; König, B.; Zeitler, K. *Angew. Chem., Int. Ed.* **2011**, *50*, 951–954.
- (19) Hari, D. P.; König, B. *Chem. Commun.* **2014**, *50*, 6688–6699.
- (20) Pelaez, M.; Nolan, N. T.; Pillai, S. C.; Seery, M. K.; Falaras, P.; Kontos, A. G.; Dunlop, P. S. M.; Hamilton, J. W. J.; Byrne, J. A.; O'shea, K.; Entezari, M. H.; Dionysiou, D. D. *Appl. Catal., B* **2012**, *125*, 331–349.
- (21) Lang, X.; Chen, X.; Zhao, J. *Chem. Soc. Rev.* **2014**, *43*, 473–486.
- (22) Moores, A.; Goettmann, F. *New J. Chem.* **2006**, *30*, 1121–1132.
- (23) Long, R.; Li, Y.; Song, L.; Xiong, Y. *Small* **2015**, *11*, 3873–3889.
- (24) Baffou, G.; Quidant, R. *Chem. Soc. Rev.* **2014**, *43*, 3898–3907.
- (25) Hwang, Y.-T.; Chung, W.-H.; Jang, Y.-R.; Kim, H.-S. *ACS Appl. Mater. Interfaces* **2016**, *8*, 8591–8599.
- (26) Dong, S.; Zhang, K.; Yu, Z.; Fan, J. A. *ACS Nano* **2016**, *10*, 6716–6724.
- (27) Jain, P. K.; Huang, X.; El-Sayed, I. H.; El-Sayed, M. A. *Plasmonics* **2007**, *2*, 107–118.
- (28) He, L.; Musick, M. D.; Nicewarner, S. R.; Salinas, F. G.; Benkovic, S. J.; Natan, M. J.; Keating, C. D. *J. Am. Chem. Soc.* **2000**, *122*, 9071–9077.
- (29) Homola, J.; Yee, S. S.; Gauglitz, G. *Sens. Actuators, B* **1999**, *54*, 3–15.
- (30) Barnes, W. L.; Dereux, A.; Ebbesen, T. W. *Nature* **2003**, *424*, 824–830.
- (31) Zhang, Y.; Manjavacas, A.; Hogan, N. J.; Zhou, L.; Ayala-Orozco, C.; Dong, L.; Day, J. K.; Nordlander, P.; Halas, N. J. *Nano Lett.* **2016**, *16*, 3373–3378.
- (32) Sharma, P.; Frontiera, R. R.; Henry, A.-I.; Ringe, E.; Van Duyne, R. P. *Mater. Today* **2012**, *15*, 16–25.
- (33) Fitch, M. T.; Silver, J. *Exp. Neurol.* **2008**, *209*, 294–301.
- (34) Guidelli, E. J.; Ramos, A. P.; Baffa, O. *Sens. Actuators, B* **2016**, *224*, 248–255.
- (35) Linic, S.; Aslam, U.; Boerigter, C.; Morabito, M. *Nat. Mater.* **2015**, *14*, 567–576.
- (36) Hou, W.; Cronin, S. B. *Adv. Funct. Mater.* **2013**, *23*, 1612–1619.
- (37) Awazu, K.; Fujimaki, M.; Rockstuhl, C.; Tominaga, J.; Murakami, H.; Ohki, Y.; Yoshida, N.; Watanabe, T. *J. Am. Chem. Soc.* **2008**, *130*, 1676–1680.
- (38) Chen, X.; Zhu, H.; Zhao, J.; Zheng, Z.; Gao, X. *Angew. Chem.* **2008**, *120*, 5433–5436.
- (39) Wang, P.; Huang, B.; Qin, X.; Zhang, X.; Dai, Y.; Wei, J.; Whangbo, M.-H. *Angew. Chem., Int. Ed.* **2008**, *47*, 7931–7933.
- (40) Tsukamoto, D.; Shiraishi, Y.; Sugano, Y.; Ichikawa, S.; Tanaka, S.; Hirai, T. *J. Am. Chem. Soc.* **2012**, *134*, 6309–6315.
- (41) Naya, S.; Inoue, A.; Tada, H. *J. Am. Chem. Soc.* **2010**, *132*, 6292–6293.
- (42) Tanaka, A.; Hashimoto, K.; Kominami, H. *Chem. Commun.* **2011**, *47*, 10446–10448.
- (43) Tan, T. H.; Scott, J.; Ng, Y. H.; Taylor, R. A.; Aguey-Zinsou, K.-F.; Amal, R. *ACS Catal.* **2016**, *6*, 1870–1879.
- (44) Naya, S.; Kimura, K.; Tada, H. *ACS Catal.* **2013**, *3*, 10–13.
- (45) Sugano, Y.; Shiraishi, Y.; Tsukamoto, D.; Ichikawa, S.; Tanaka, S.; Hirai, T. *Angew. Chem., Int. Ed.* **2013**, *52*, 5295–5299.
- (46) Sarina, S.; Zhu, H.; Jaatinen, E.; Xiao, Q.; Liu, H.; Jia, J.; Chen, C.; Zhao, J. *J. Am. Chem. Soc.* **2013**, *135*, 5793–5801.
- (47) González-Béjar, M.; Peters, K.; Hallett-Tapley, G. L.; Grenier, M.; Scaiano, J. C. *Chem. Commun.* **2013**, *49*, 1732–1734.
- (48) Naya, S.; Nikawa, T.; Kimura, K.; Tada, H. *ACS Catal.* **2013**, *3*, 903–907.

- (49) Pineda, A.; Gomez, L.; Balu, A. M.; Sebastian, V.; Ojeda, M.; Arruebo, M.; Romero, A. A.; Santamaria, J.; Luque, R. *Green Chem.* **2013**, *15*, 2043–2049.
- (50) Zheng, Z.; Huang, B.; Qin, X.; Zhang, X.; Dai, Y.; Whangbo, M.-H. *J. Mater. Chem.* **2011**, *21*, 9079–9087.
- (51) Ide, Y.; Matsuoka, M.; Ogawa, M. *J. Am. Chem. Soc.* **2010**, *132*, 16762–16764.
- (52) Ide, Y.; Nakamura, N.; Hattori, H.; Ogino, R.; Ogawa, M.; Sadakane, M.; Sano, T. *Chem. Commun.* **2011**, *47*, 11531–11533.
- (53) Christopher, P.; Xin, H.; Linic, S. *Nat. Chem.* **2011**, *3*, 467–472.
- (54) Wang, F.; Li, C.; Chen, H.; Jiang, R.; Sun, L.-D.; Li, Q.; Wang, J.; Yu, J. C.; Yan, C.-H. *J. Am. Chem. Soc.* **2013**, *135*, 5588–5601.
- (55) McClain, M. J.; Schlather, A. E.; Ringe, E.; King, N. S.; Liu, L.; Manjavacas, A.; Knight, M. W.; Kumar, I.; Whitmire, K. H.; Everitt, H. O.; Nordlander, P.; Halas, N. J. *Nano Lett.* **2015**, *15*, 2751–2755.
- (56) Swearer, D. F.; Zhao, H.; Zhou, L.; Zhang, C.; Robotjazi, H.; Martirez, J. M. P.; Krauter, C. M.; Yazdi, S.; McClain, M. J.; Ringe, E.; Carter, E. A.; Nordlander, P.; Halas, N. J. *Proc. Natl. Acad. Sci. U. S. A.* **2016**, *113*, 8916–8920.
- (57) Kim, C.; Suh, B. L.; Yun, H.; Kim, J.; Lee, H. *ACS Catal.* **2017**, *7*, 2294–2302.
- (58) da Silva, A. G. M.; Rodrigues, T. S.; Correia, V. G.; Alves, T. V.; Alves, R. S.; Ando, R. A.; Ornellas, F. R.; Wang, J.; Andrade, L. H.; Camargo, P. H. C. *Angew. Chem., Int. Ed.* **2016**, *55*, 7111–7115.
- (59) Zhao, L.-B.; Liu, X.-X.; Zhang, M.; Liu, Z.-F.; Wu, D.-Y.; Tian, Z.-Q. *J. Phys. Chem. C* **2016**, *120*, 944–955.
- (60) Martirez, J. M. P.; Carter, E. A. *ACS Nano* **2016**, *10*, 2940–2949.
- (61) van Schroyen Lantman, E. M.; Deckert-Gaudig, T.; Mank, A. J.; Deckert, V.; Weckhuysen, B. M. *Nat. Nanotechnol.* **2012**, *7*, 583–586.
- (62) Hallett-Tapley, G. L.; Silvero, M. J.; González-Béjar, M.; Grenier, M.; Netto-Ferreira, J. C.; Scaiano, J. C. *J. Phys. Chem. C* **2011**, *115*, 10784–10790.
- (63) Marimuthu, A.; Zhang, J.; Linic, S. *Science* **2013**, *339*, 1590–1593.
- (64) de Vries, J. G.; Elsevier, C. J. *The Handbook of Homogeneous Hydrogenation*; Wiley-VCH: Weinheim, 2007; pp 1–30.
- (65) Claus, P. *Top. Catal.* **1998**, *5*, 51–62.
- (66) Mäki-Arvela, P.; Hájek, J.; Salmi, T.; Murzin, D. Y. *Appl. Catal., A* **2005**, *292*, 1–49.
- (67) Zheng, J.; Duan, X.; Lin, H.; Gu, Z.; Fang, H.; Li, J.; Yuan, Y. *Nanoscale* **2016**, *8*, 5959–5967.
- (68) Yang, L.; Xing, L.; Cheng, C.; Xia, L.; Liu, H. *RSC Adv.* **2016**, *6*, 31871–31875.
- (69) Jia, Z.; Zhou, F.; Liu, M.; Li, X.; Chan, A. S. C.; Li, C.-J. *Angew. Chem., Int. Ed.* **2013**, *52*, 11871–11874.
- (70) Mukherjee, S.; Libisch, F.; Large, N.; Neumann, O.; Brown, L. V.; Cheng, J.; Lassiter, J. B.; Carter, E. A.; Nordlander, P.; Halas, N. J. *Nano Lett.* **2013**, *13*, 240–247.
- (71) Mukherjee, S.; Zhou, L.; Goodman, A. M.; Large, N.; Ayala-Orozco, C.; Zhang, Y.; Nordlander, P.; Halas, N. J. *J. Am. Chem. Soc.* **2014**, *136*, 64–67.
- (72) Wiley, B. J.; Im, S. H.; Li, Z.-Y.; McLellan, J.; Siekkinen, A.; Xia, Y. *J. Phys. Chem. B* **2006**, *110*, 15666–15675.
- (73) Lachheb, H.; Puzenat, E.; Houas, A.; Ksibi, M.; Elaloui, E.; Guillard, C.; Herrmann, J.-M. *Appl. Catal., B* **2002**, *39*, 75–90.
- (74) Wiley, B.; Sun, Y.; Mayers, B.; Xia, Y. *Chem. - Eur. J.* **2005**, *11*, 454–463.
- (75) Li, A. Y.; Kaushik, M.; Li, C.-J.; Moores, A. *ACS Sustainable Chem. Eng.* **2016**, *4*, 965–973.
- (76) Mukherjee, S.; Vannice, A. J. *Catal.* **2006**, *243*, 108–130.
- (77) Christopher, P.; Xin, H.; Marimuthu, A.; Linic, S. *Nat. Mater.* **2012**, *11*, 1044–1050.
- (78) Horiuti, I.; Polanyi, M. *Trans. Faraday Soc.* **1934**, *30*, 1164–1172.
- (79) Yan, J.; Jacobsen, K. W.; Thygesen, K. S. *Phys. Rev. B: Condens. Matter Mater. Phys.* **2011**, *84*, 235430.
- (80) Yang, Y.; Zhao, Y.; Yan, Y.; Wang, Y.; Guo, C.; Zhang, J. *J. Phys. Chem. B* **2015**, *119*, 14807–14813.
- (81) Wang, P.; Huang, B.; Qin, X.; Zhang, X.; Dai, Y.; Wei, J.; Whangbo, M.-H. *Angew. Chem., Int. Ed.* **2008**, *47*, 7931–7933.
- (82) Han, L.; Wang, P.; Zhu, C.; Zhai, Y.; Dong, S. *Nanoscale* **2011**, *3*, 2931–2935.